Biomol NMR Assign (2015) 9:81–88
DOI 10.1007/s12104-014-9549-z

ARTICLE

Assignments of RNase A by ADAPT-NMR and enhancer

Marco Tonelli · Chelcie H. Eller · Kiran K. Singarapu · Woonghee Lee · Arash Bahrami · William M. Westler · Ronald T. Raines · John L. Markley

Received: 10 October 2013 / Accepted: 28 February 2014 / Published online: 12 March 2014

Abstract We report here backbone ^{1}H and ^{15}N assignments for ribonuclease A obtained by using ADAPT-NMR, a fully-automated approach for combined data collection, spectral analysis and resonance assignment. ADAPT-NMR was able to assign 98 % of the resonances with 93 % agreement with traditional data collection and assignment. Further refinement of the automated results with ADAPT-NMR enhancer led to complete (100 %) assignments with 96 % agreement with assignments by the traditional approach.

Keywords RNase A · Cancer chemotherapy · Automated protein NMR assignments · ADAPT-NMR · ADAPT-NMR enhancer

Electronic supplementary material The online version of this article (doi:10.1007/s12104-014-9549-z) contains supplementary material, which is available to authorized users.

M. Tonelli (✉) · K. K. Singarapu · W. Lee · A. Bahrami · W. M. Westler · J. L. Markley
National Magnetic Resonance Facility at Madison, University of Wisconsin – Madison, 433 Babcock Drive, Madison, WI 53706, USA
e-mail: tonelli@nmrfam.wisc.edu

C. H. Eller · W. Lee · R. T. Raines · J. L. Markley
Department of Biochemistry, University of Wisconsin – Madison, 433 Babcock Drive, Madison, WI 53706, USA

Present Address:
K. K. Singarapu
Center for NMR and Structural Chemistry, CSIR, Indian Institute of Chemical Technology, Uppal Road, Tarnaka, Hyderabad 500007, India

R. T. Raines
Department of Chemistry, University of Wisconsin – Madison, 1101 University Avenue, Madison, WI 53706, USA

Biological context

Bovine pancreatic ribonuclease (RNase A) is a 124-residue protein that has served as a model for much landmark work on protein structure and function. RNase A is the third enzyme whose structure was determined by X-ray crystallography and is now the subject of more than 30 PDB entries. In addition, RNase A played a crucial role in the early development of NMR spectroscopy, leading to the determination of its solution structure (for a review, see: Raines 1998). RNase A catalyzes the cleavage of the P–O$^{5'}$ bond of RNA with a k_{cat}/K_M value that can exceed 10^9 M^{-1} s^{-1} and exhibits high thermostability (T_m 62 °C) (for a review, see: Lomax et al. 2012). The presumed biological function of RNase A is catalysis of the depolymerization of ingested RNA. Yet, high levels of RNase A and its human homologue (RNase 1) in many different tissues are consistent with additional roles (Futami et al. 1997; Wheeler et al. 2012).

Recently, homologs and variants of RNase A have shown potential as cancer chemotherapeutic agents (Lomax et al. 2012). Enabling RNase A to achieve its clinical potential is likely to require a thorough understanding of its interactions with cellular molecules, including cell-surface glycans and the cytosolic ribonuclease inhibitor protein. Structural and dynamic aspects of these interactions can be probed by NMR spectroscopy. While characterizing these interactions, we found that our ^{1}H–^{15}N backbone assignments did not match with those reported previously (Shimotakahara et al. 1997). In particular, assignments to several amide peaks in flexible loop regions varied, despite the use of identical buffer conditions. We used the ADAPT-NMR method (Bahrami et al. 2012; Lee et al. 2013a, b) to assign the backbone amide resonances. Then, we confirmed these assignments by a

more traditional manual approach. The ensuing information adds to the history of RNase A and provides the basis for further analyses.

Experimental procedures

Production of [^{13}C, ^{15}N]RNase A

[^{13}C, ^{15}N]-RNase A was produced by heterologous expression in *Escherichia coli* strain BL21(DE3) as described previously (Johnson et al. 2007), with the exception of a double growth protocol in minimal medium. Induction medium contained 0.13 % w/v [^{15}N]-NH_4Cl and 0.4 % w/v [U-^{13}C6]-D-glucose (Cambridge Isotope Laboratories, Andover, MA, USA) for isotope incorporation upon addition of IPTG (Sigma-Aldrich, St. Louis, MO, USA) to 0.5 mM. Protein purification was monitored with SDS-PAGE. The mass of the final purified product was determined with matrix-assisted laser desorption/ionization (MALDI) mass spectroscopy at the University of Wisconsin Biotechnology Center. RNase A has the molecular formula $C_{575}H_{901}N_{171}O_{193}S_{12}$ and a molecular mass of 13,682 Da. The observed mass of 14,317 Da indicated a level of isotope incorporation of $(14{,}317 - 13{,}682)/(575 + 171) = 85$ %.

To confirm that protein function was not compromised upon labeling, RNase A was assayed for ribonucleolytic activity by using a fluorogenic substrate, 6-FAM–dArUdGdA–6-TAMRA (Integrated DNA Technologies, Coralville, IA, USA) (Lomax et al. 2012). Upon cleavage of this substrate at ambient temperature, excitation at 492 nm elicits fluorescence at 515 nm. Assays were performed in oligo(vinylsulfonic acid)-free 0.10 M MES–NaOH buffer, pH 6.0 containing NaCl (0.10 M). The catalytic activity of the labeled RNase A [$k_{cat}/K_M = (14.5 \pm 3.5)\ \mu M^{-1}\ s^{-1}$] was indistinguishable from that of unlabeled RNase A [$k_{cat}/K_M = (21.6 \pm 7.9)\ \mu M^{-1}\ s^{-1}$].

Preparation of NMR samples

For chemical shift assignments, freshly prepared RNase A was dialyzed into water, lyophilized, and dissolved in 100 mM potassium phosphate buffer, pH 4.7, containing 10 % D_2O (Sigma-Aldrich) to a final protein concentration of 1.7 mM. Another sample of RNase A was dissolved in 90:10 H_2O:D_2O at pH 4.7 to reproduce conditions from previously determined assignments (Shimotakahara et al. 1997). This sample was used to carry out a titration experiment with potassium phosphate also at pH 4.7. Samples used for NMR spectroscopy were enclosed in 5-mm susceptibility-matched Shigemi NMR tubes (Shigemi, Allison Park, PA, USA).

NMR data collection

All NMR spectra were acquired on Varian VNMRS spectrometers (Agilent Technologies, Santa Clara, CA, USA) equipped with cryogenic triple-resonance probes. Two types of data collection and analysis were performed: traditional and fully automated using ADAPT-NMR (Bahrami et al. 2012). For the traditional assignment approach, 2D ^{1}H, ^{15}N-HSQC, 3D HNCACB and 3D NOESY ^{15}N-HSQC spectra were collected at 900 MHz (^{1}H) with the temperature of the sample regulated at 293 K (Table 1). Peak lists generated from 2D ^{1}H, ^{15}N-HSQC and 3D HNCACB spectra were fed to the PINE server (Bahrami et al. 2009), and the assignments obtained were further refined by hand by reference to a 3D ^{15}N-resolved ^{1}H–^{1}H NOESY spectrum viewed with Sparky (Goddard and Kneller 2000).

For fully automated backbone assignments with ADAPT-NMR, in addition to a 2D ^{1}H–^{15}N HSQC spectrum, six 3D spectra were collected as 2D planes: HNCO, HN(CA)CO, HN(CO)CA, HNCA, CBCA(CO)NH and HN(CA)CB. All spectra were collected at 600 MHz (^{1}H) at 308 K (Table 2). The pulse programs for these experiments were taken from BioPack (Varian/Agilent) and adapted for reduced dimensionality data collection as previously described (Bahrami et al. 2012). All orthogonal and tilted planes were processed automatically by ADAPT-NMR with NMRpipe software (Delaglio et al. 1995). The fully automated assignments were visualized, validated and further refined by using the ADAPT-NMR enhancer package (Lee et al. 2013a). To reconcile assignments from the manual and ADAPT-NMR approaches, a series of 2D ^{1}H, ^{15}N-HSQC spectra were collected at temperatures ranging from 293 to 308 K at 2.5 K intervals (Table 3).

Table 1 Experimental details for 3D spectra collected for conventional assignments

Experiment	Spectral window (KHz) ^{1}H × ^{13}C(^{1}H*) × ^{15}N	# Scans	Complex points	Time
HNCACB	14.5 × 18.1 × 2.7	4	1,024 × 96 × 48	23 h 5 min
^{1}H–^{1}H NOESY ^{15}N-HSQC	14.5 × 12* × 2.7	8	1,024 × 96 × 48	49 h 4 min

All spectra were collected with a cryogenic probe at 900 MHz (^{1}H) at a temperature of 293 K

Table 2 Experimental details for all 2D spectra collected by ADAPT-NMR

Experiment	Tilt angles of collected Planes	Spectral window (KHz) $^{1}H \times ^{13}C \times ^{15}N$	# Scans	Complex points	Time/ tilted plane	Time/0° plane
HNCO	25, 60, 69	10 × 2.2 × 2.2	4	1,024 × 96	32 min	16 min
HN(CA)CO	28, 34, 41, 53, 69	10 × 2.2 × 2.2	16	1,024 × 96	2 h 6 min	1 h 3 min
HN(CO)CA	28, 40, 64	10 × 4.8 × 2.2	8	1,024 × 96	1 h 3 min	32 min
HNCA	26, 40, 51, 58, 56	10 × 4.8 × 2.2	8	1,024 × 96	1 h 2 min	31 min
CBCA(CO)NH	25, 32, 43, 50, 57	10 × 11.2 × 2.2	16	1,024 × 55	1 h 10 min	33 min
HN(CA)CB	12, 14, 15, 17, 18, 19, 22, 26, 29, 31, 32, 34, 37, 38, 47, 58, 66	10 × 11.2 × 2.2	16	1,024 × 128	2 h 47 min	1 h 24 min

All spectra were collected with a cryogenic probe at 600 MHz (^{1}H) at 308 K. A 2D ^{1}H–^{15}N HSQC spectrum was used as the 90° tilted plane in each experiment

Table 3 Experimental details for 600 MHz (^{1}H) 2D spectra acquired with a cryogenic probe as a function of temperature

Experiment	Temperature (K)	Spectral window (KHz) $^{1}H \times ^{15}N$	# scans	Complex points	Time
^{1}H–^{15}N HSQC	293, 295.5, 298, 300.5, 303, 305.5, 308	10 × 2.2	8	1,024 × 256	1 h 29′

Table 4 Experimental details for 800 MHz (^{1}H) 2D spectra collected with a conventional probe as a function of added potassium phosphate

Experiment	Potassium phosphate concentration (mM)	Spectral window (kHz) $^{1}H \times ^{15}N$	# Scans	Complex points	Time/ spectrum
^{1}H–^{15}N HSQC	0, 0.25, 0.75, 1.25, 2.5, 6.25, 11.25, 21.25, 40	13 × 2.8	8	512 × 256	1 h 20 min

An in-house written macro was used to collect these experiments in an automated fashion.

Finally, potassium phosphate was titrated into a solution of 0.25 mM ^{15}N-labeled RNase A dissolved in 90:10 H_2O:D_2O at pH 4.7, and 2D ^{1}H–^{15}N HSQC spectra were collected after each addition. These spectra were acquired on a Varian VNMRS spectrometer operating at 800 MHz (^{1}H) equipped with a conventional triple-resonance, triple-axis gradient probe (Table 4) with the temperature of the sample regulated at 293 K. Including the starting point, a total of nine spectra were acquired at increasing phosphate concentrations: 0, 0.250, 0.750, 1.25, 2.50, 6.25, 11.25, 21.25 and 40.0 mM, corresponding to phosphate:RNase A molar ratios of 0:1, 1:1, 3:1, 5:1, 10:1, 25:1, 45:1, 85:1 and 160:1, respectively. All 2D spectra were processed by NMRPipe and analyzed with Sparky.

NMR assignments and data deposition

NMR backbone assignments: ADAPT-NMR versus traditional

In our aim to study the interaction of potential cancer chemotherapeutic agents to cell-surface moieties by NMR, we prepared an ^{15}N-labeled sample of RNase A and planned to use the assignments deposited in BMRB (BMRB ID 4031) to identify the peaks in the 2D ^{1}H, ^{15}N-HSQC spectra. However, even though we adjusted the sample conditions to match those reported in BMRB (H_2O, pH 4.6 293 K), the deposited assignments did not agree with the peaks in our spectra. Thus, we prepared a doubly labeled (^{15}N, ^{13}C) sample and assigned the protein backbone signals by using ADAPT-NMR, the fully automated approach for data collection, processing and analysis developed in our laboratory. The ADAPT-NMR approach made use of six 3D experiments collected as 2D tilted planes: HNCO, HN(CA)CO, HN(CO)CA, HNCA, CBCA(CO)NH and HN(CA)CB. The tilted angles and experiments selected on-the-fly by ADAPT-NMR for data collection and other experimental details are provided in Table 2. Of these experiments, HN(CA)CB is the least sensitive and the most complicated spectrum to analyze, and, not surprisingly, it is also the one that took the longest time to collect. Thus, whereas data collection for the first five 3D experiments in the list took 32 h, the HN(CA)CB experiment alone required 17 tilted planes and an additional 48 h to collect. In the end, without any intervention by the user, ADAPT-NMR succeeded in assigning 117 of the 119 assignable residues (124 total residues minus the

Table 5 Comparison between manual assignments and automated assignments made by ADAPT-NMR before and after use of the ADAPT-NMR enhancer package

	Manual assignments	ADAPT-NMR assignments	ADAPT-NMR enhancer assignments
Manual assignments	94 % (I81–D83, Q101–Q102, H119–F120)	E2, S16–A19, S23–S23, C84	A19, S22, C84, G112, N113
ADAPT-NMR assignments	93 %	98 % (V63, K66)	E2, S16–S18, S23–S23, G112, N113
ADAPT-NMR enhancer assignments	96 %	93 %	100 %

The cells along the diagonal show the percent of assigned residues achieved by each of the three methods, along with a list (in parentheses) of the residues that were not assigned. The top/right portion of the table lists the residues whose assignments differed between the methods at each intersection. The bottom/left portion reports the percent agreement between the methods at each intersection

N-terminal residue and 4 prolines) for an assignment completion of 98 % (only V63 and K66 were not assigned by ADAPT-NMR). Of these 117 residues, 113 were assigned with a probability score of above 80 %.

Subsequently, in order to gather better and more complete assignments, the results of ADAPT-NMR were visualized and validated by using the ADAPT-NMR enhancer package (Lee et al. 2013a). Using this package according to the procedure described in the supplementary material, we generated new and improved peak lists and reran ADAPT-NMR. The program automatically detected the user-modified peak lists, and tried to find better assignments without collecting any additional NMR spectra. In the end, all 119 possible amino acids were identified by ADAPT-NMR, and the assignments for eight residues, E2, S16–S18, S22–S23, G112–N113, were changed relative to those obtained by the automated approach prior to refinement with enhancer (Table 5).

As a means of verifying the assignments made by ADAPT-NMR, we submitted peak lists generated with Sparky from 2D ^{1}H–^{15}N HSQC and 3D HNCACB spectra to the PINE server (Bahrami et al. 2009), and refined the resulting assignments by hand with reference to the ^{15}N-resolved ^{1}H–^{1}H NOESY 3D spectrum as displayed by Sparky (Goddard and Kneller 2000). Using this approach, we were able to assign signals to 112 residues (out of 119 assignable residues—94 % completion). The remaining residues could not be identified because of ambiguities that we could not resolve using the spectra at our disposal.

To reconcile the automated assignments by ADAPT-NMR carried out at 308 K with the traditional assignments from 3D spectra collected at 293 K, we collected a series of 2D ^{1}H–^{15}N HSQC spectra at 2.5° intervals between 293

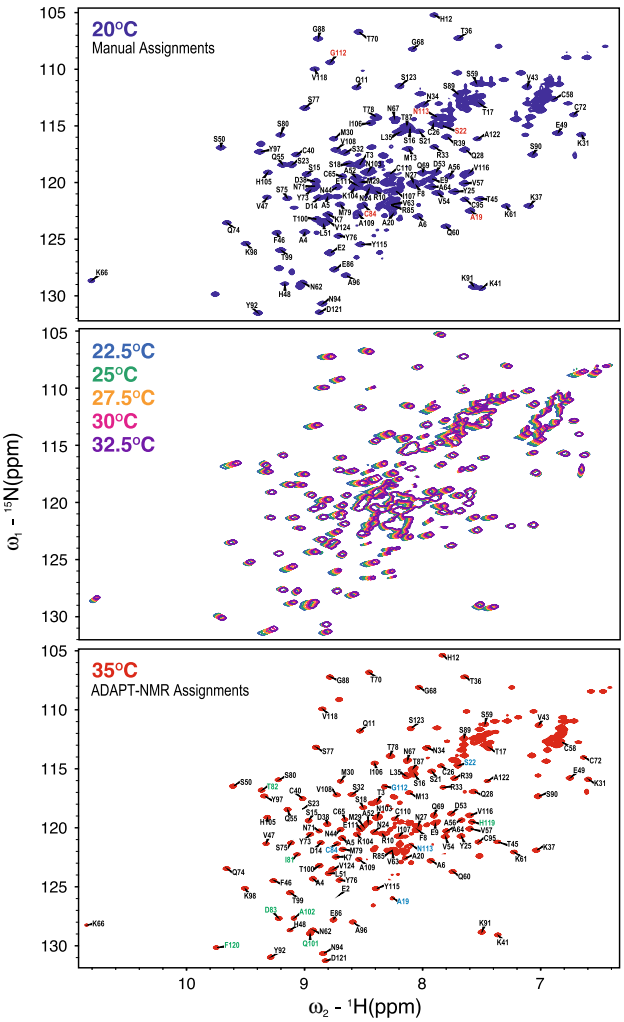

Fig. 1 Temperature dependence of 2D ^{1}H–^{15}N HSQC spectra of RNase A. The spectrum recorded at 293 K is shown in the *top panel*. *Peaks* are labeled with the backbone assignments obtained by the traditional approach (residues whose assignment is different from the automated approach are labeled in *red*). *Bottom panel* shows the spectrum recorded at 308 K with enhancer-refined ADAPT-NMR assignments (residues that were assigned by ADAPT-NMR but not the traditional approach are labeled in *green*; residues whose assignment is different from the traditional one are labeled in *cyan*). In the *middle panel* the 2D ^{1}H–^{15}N HSQC spectra recorded at temperatures ranging from 295.5 to 305.5 K are shown color-coded. As reported in Table 3, the spectra were collected on a Varian VNMRS spectrometer, operating at 600 MHz, equipped with a cryogenic *z* axis gradient probe

and 208 K. For residues identified by both methods, this analysis yielded 93 % agreement between the assignments made by ADAPT-NMR and those from our limited traditional approach (102 out of the 110 commonly assigned residues). The agreement with the manual assignments increased to 96 % (107 out of 112 common assignments) after the enhancer package was used to refine the ADAPT-NMR results. In the end, only the ADAPT-NMR assignments for A19, S22, C84, G112 and N113 were

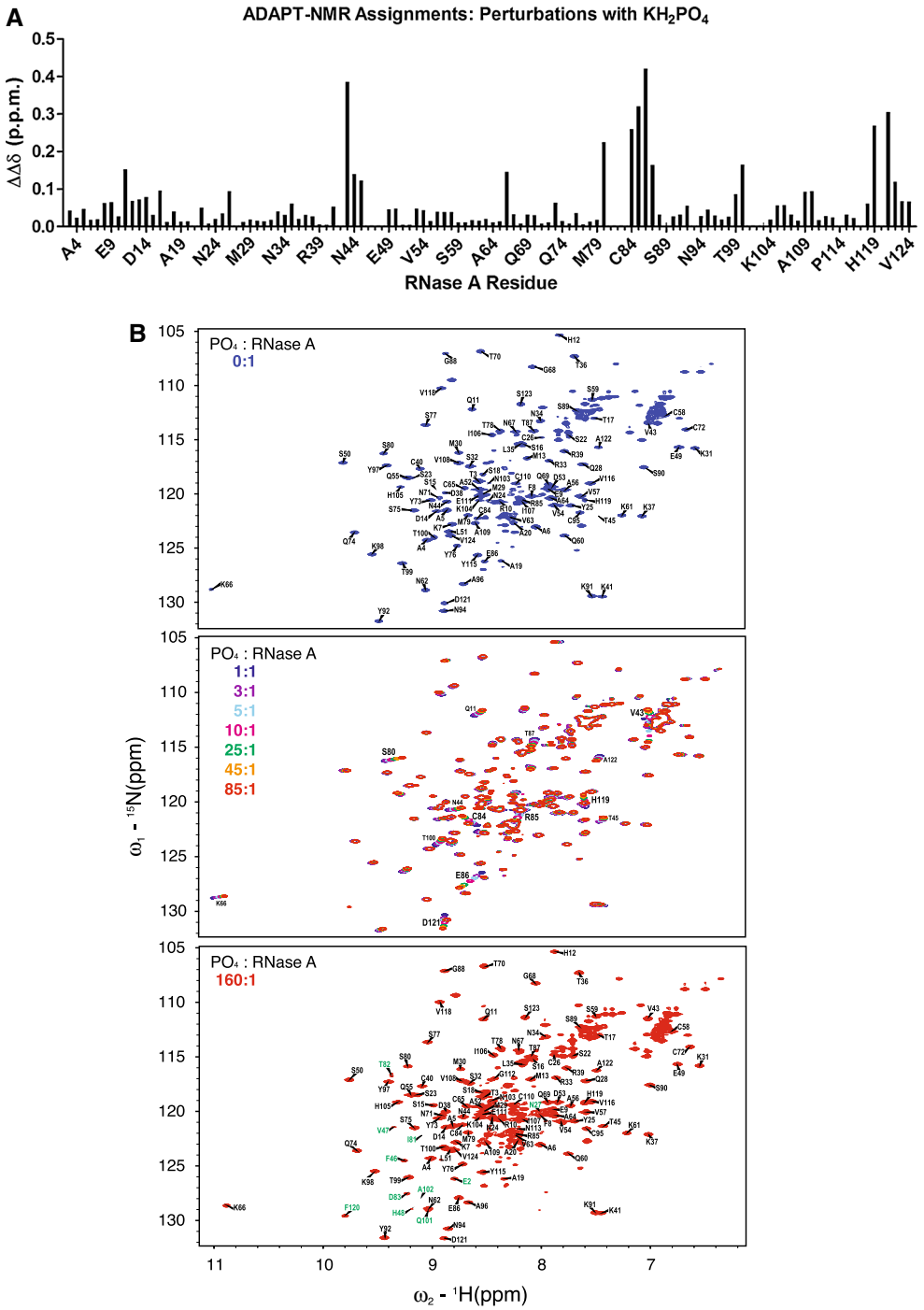

Fig. 2 Effect of phosphate on the backbone $^{1}H–^{15}N$ chemical shifts of RNase A. Data were collected from RNase A samples at pH 4.7 in the absence of phosphate and in the presence of 40 mM potassium phosphate. 2D $^{1}H–^{15}N$ HSQC spectra were collected at 273 K on a Varian VNMR 800 MHz spectrometer equipped with a triple-axis gradient conventional probe. **A** Differences in the backbone $^{1}H–^{15}N$ chemical shifts of RNase A in the absence of phosphate and in the presence of 40 mM potassium phosphate. Chemical shift differences ($\Delta\Delta\delta$) were calculated from the equation $(\Delta\Delta\delta) = ((\Delta\delta^{1}H)^{2} + 1/5(\Delta\delta^{15}N)^{2})^{1/2}$. Known nucleotide phosphate binding residues are K7, R10, K66, R85, while phosphate binding residues are Q11, H12, K41, H119, F120. **B** Phosphate titration spectra. The *top panel* shows a 2D $^{1}H–^{15}N$ HSQC spectrum recorded in the absence of phosphate. The *bottom panel* reports the spectrum recorded at the end of the phosphate titration. *Peaks* that were too broad to be visible in the absence of phosphate are labeled in *green*. The *middle panel* shows color-coded and overlapped spectra from the intermediate phosphate titration points. Residues that undergo the largest chemical shift changes upon the addition of phosphate are labeled (with a bigger font for those with the largest shifts)

inconsistent with those from the manual method. The enhancer treatment left those for A19 and C84 unchanged and reconciled the assignments for S16–S18 and S23 with the manual ones, but its change in the assignment for S22 continued to be different from the manual assignment. Careful inspection of the peak connectivities for A19 and C84 suggested that the assignments found for these residues by ADAPT-NMR are more likely correct than the manual ones. In particular, C84 follows a string of residues that were not identified by the traditional method, thus rendering its assignment by ADAPT-NMR more reliable. On the other hand, the assignment for S22 was changed to a peak located within the ADAPT-NMR chemical shift tolerance of the peak assigned by the manual approach. Finally, the enhancer treatment also altered the ADAPT-NMR assignments for residues G112 and N113 that initially agreed with the manual ones. It is likely that the expanded peak lists generated after using the enhancer package provided ADAPT-NMR with more probable assignments for these residues.

In any case, ADAPT-NMR was able to assign signals to seven more residues (I81–D83, Q101–A102, H119–F120) than the manual approach (Table 5). The temperature titration spectra with both ADAPT-NMR and traditional assignments are shown in Fig. 1. We have deposited the assignments made by ADAPT-NMR/enhancer and by the traditional approach along with the assigned $^{1}H–^{15}N$ peak lists determined as a function of temperature (BMRB ID number 19065).

Effect of phosphate on RNase A

To investigate the effect of phosphate on RNase A, we added increasing amounts of potassium phosphate to a solution of RNase A at 293 K and pH 4.7. At each titration point, we collected a 2D $^{1}H–^{15}N$ HSQC spectrum and used these spectra, along with the our ADAPT-NMR assignments obtained at 308 K in the presence of phosphate buffer and extrapolated to the same temperature by means of the temperature titration data, to extract the assignments for RNase A in the absence of phosphate. We observed that, whereas most peaks shifted upon the addition of phosphate, some shifted much more than others. As shown in Fig. 2, peaks from residues V43, S80, C84, R85, E86, H119 and D121 showed the largest chemical shift changes upon the addition of phosphate, followed by Q11, N44, T45, K66, T87, T100 and A122. The majority of these peaks are in discrete regions of the protein, located near residues that are known to bind phosphate (Q11, H12, K41, H119, F120) or nucleotide phosphate (K7, R10, K66, R85) (Wlodawer et al. 1986). These residues are in general agreement with residues perturbed by sodium phosphate buffer (Wong et al. 2013). Furthermore, with the addition of phosphate, $^{1}H–^{15}N$ HSQC cross peaks generally sharpened, in particular those that exhibited the largest chemical shift perturbations. Peaks from residues E2, S21, N27, F46–H48, I81–D83, Q101–A102 and F120 were too broad to be observed in the absence of phosphate. This broadening suggests the presence of

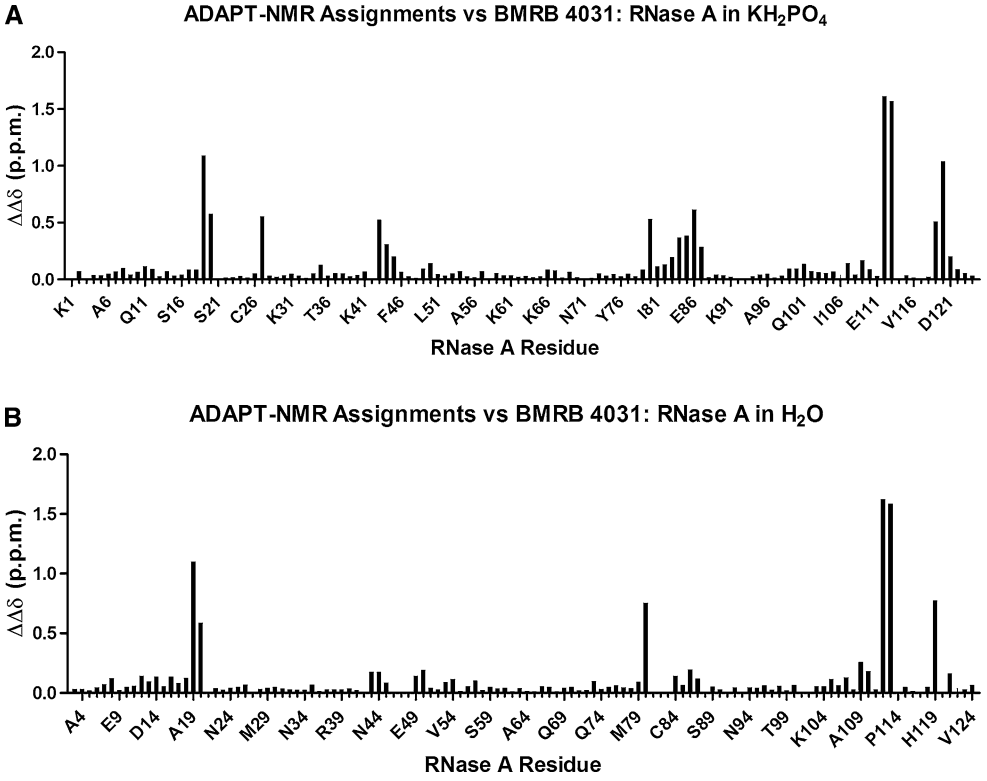

Fig. 3 **A** Comparison between RNase A assignments by ADAPT-NMR in the presence of 40 mM phosphate (160:1 molar ratio to RNase A) and assignments deposited in BMRB (BMRB ID 4031). **B** Comparison between RNase A assignments in the absence of phosphate and BMRB ID 4031 assignments. All chemical shift perturbations (ΔΔδ) were calculated from the equation $(\Delta\Delta\delta) = ((\Delta\delta^{1}H)^{2} + 1/5(\Delta\delta^{15}N)^{2})^{1/2}$

conformational dynamic processes on the intermediate NMR time scale that are reduced upon binding of phosphate. The assigned backbone ^{1}H and ^{15}N chemical shifts for RNase A extrapolated to zero phosphate have been deposited at BMRB along with assigned peak lists at each phosphorus concentration (ID 19065). Our assignments at the end of the titration (40 mM phosphate) were still slightly different from those we obtained with the sample dissolved in 100 mM phosphate buffer (average $\Delta\Delta\delta$ of 0.0227 $\pm$ 0.0119 ppm).

Comparison with assignments deposited in BMRB

The previous assignments for RNase A (Shimotakahara et al. 1997) were determined with a protein sample in the absence of phosphate. Thus, it is not surprising that our assignments for RNase A in the presence of 100 mM phosphate differed, particularly for residues known to bind phosphate (V43–T45 and C84–T87) (Fig. 3a). Still, to our surprise, we found that many of our assignments in the absence of phosphate also did not match the deposited ones, although the discrepancies were fewer (Fig. 3b). The origin of these differences is unclear. Because previous reports had suggested that deamidation of Asn and Gln side chains at multiple sites could be a possible source of variability in RNase A (Esposito et al. 2000; Zabrouskov et al. 2006), we inspected the 2D ^{1}H–^{15}N HSQC peaks from the side-chain NH_2 groups of Asn and Gln. We found the correct number of peaks for RNase A, suggesting that deamidation had not taken place in our sample. Deamidation of the previous sample seems unlikely, as N67, the more predominant site of modification (Zabrouskov et al. 2006), or neighboring residues 66–69 were not major sites of discrepancy. Still, changes between assignments were observed at N113 and neighboring residue, G112. The sample preparation from Shimotakahara exposed RNase A to disodium 2-nitro-5-(sulfothio)benzoate, and subsequent refolding occurred in a buffer of pH 8.2 (Laity et al. 1993). Current methods of RNase A purification do not subject the protein to such harsh and basic conditions. It is possible, for example, that the oxidizing agent intended for cysteine residues resulted in covalent modification of the side chains of serines, threonines, or lysines. Indeed, sites of changes that were observed between both the ADAPT-NMR and manual assignments to BMRB 4031 were residues positioned within serine-rich loop region S15–S23 and S80. The previously referenced method also measured catalytic activity using an insensitive assay that might not have detected damage to the enzyme.

In conclusion, fully automated ADAPT-NMR achieved an assignment level of 98 % for RNase A in the presence of 100 mM phosphate buffer; the assignments were refined and brought to a level of 100 % by use of the ADAPT-NMR enhancer package. These levels of assignment were greater than that achieved by a more traditional approach, albeit with a more limited set of data. As described previously (Shimotakahara et al. 1997), spectra of RNase A contain signals from minor conformational states. It appears that these additional peaks, which can be linked together in data from triple-resonance backbone experiments, misled somewhat the automated assignments carried out by ADAPT-NMR. These errors could be rectified by use of the enhancer package to achieve complete assignments.

Acknowledgments This study was supported by NIH Grant R01 CA073808 (NCI) and made use of the National Magnetic Resonance Facility at Madison, with support from NIH Grants P41 RR02301 (BRTP/NCRR) and P41 GM66326 (BRTP/NIGMS). Additional equipment was purchased with funds from the University of Wisconsin, the NIH (RR02781, RR08438), the NSF (DMB-8415048, OIA-9977486, BIR-9214394), and the USDA.

References

Bahrami A, Assadi AH, Markley JL, Eghbalnia HR (2009) Probabilistic interaction network of evidence algorithm and its application to complete labeling of peak lists from protein NMR spectroscopy. PLoS Comput Biol 5(3):e1000307. doi:10.1371/journal.pcbi.1000307

Bahrami A, Tonelli M, Sahu SC, Singarapu KK, Eghbalnia HR, Markley JL (2012) Robust, integrated computational control of NMR experiments to achieve optimal assignment by ADAPT-NMR. PLoS One 7(3):e33173. doi:10.1371/journal.pone.0033173

Delaglio F, Grzesiek S, Vuister GW, Zhu G, Pfeifer J, Bax A (1995) Nmrpipe: a multidimensional spectral processing system based on unix pipes. J Biomol NMR 6(3):277–293. doi:10.1007/Bf00197809

Esposito L, Vitagliano L, Sica F, Sorrentino G, Zagari A, Mazzarella L (2000) The ultrahigh resolution crystal structure of ribonuclease A containing an isoaspartyl residue: hydration and stereochemical analysis. J Mol Biol 297(3):713–732. doi:10.1006/jmbi.2000.3597

Futami J, Tsushima Y, Murato Y, Tada H, Sasaki J, Seno M, Yamada H (1997) Tissue-specific expression of pancreatic-type RNases and RNase inhibitor in humans. DNA Cell Biol 16(4):413–419. doi:10.1089/dna.1997.16.413

Goddard TD, Kneller DG (2000) SPARKY 3. University of California, San Francisco

Johnson RJ, McCoy JG, Bingman CA, Phillips GN Jr, Raines RT (2007) Inhibition of human pancreatic ribonuclease by the human ribonuclease inhibitor protein. J Mol Biol 368(2):434–449. doi:10.1016/j.jmb.2007.02.005

Laity JH, Shimotakahara S, Scheraga HA (1993) Expression of wild-type and mutant bovine pancreatic ribonuclease A in *Escherichia coli*. Proc Natl Acad Sci USA 90(2):615–619

Lee W, Bahrami A, Markley JL (2013a) ADAPT-NMR enhancer: complete package for reduced dimensionality in protein NMR spectroscopy. Bioinformatics 29(4):515–517. doi:10.1093/bioinformatics/bts692

Lee W, Hu K, Tonelli M, Bahrami A, Neuhardt E, Glass KC, Markley JL (2013b) Fast automated protein NMR data collection and assignment by ADAPT-NMR on Bruker spectrometers. J Magn Reson 236:83–88. doi:10.1016/j.jmr.2013.08.010

Lomax JE, Eller CH, Raines RT (2012) Rational design and evaluation of mammalian ribonuclease cytotoxins. Method Enzym 502:273–290. doi:10.1016/B978-0-12-416039-2.00014-8

Raines RT (1998) Ribonuclease A. Chem Rev 98(3):1045–1066. doi:10.1021/cr960427h

Shimotakahara S, Rios CB, Laity JH, Zimmerman DE, Scheraga HA, Montelione GT (1997) NMR structural analysis of an analog of an intermediate formed in the rate-determining step of one pathway in the oxidative folding of bovine pancreatic ribonuclease A: automated analysis of ^{1}H, ^{13}C, and ^{15}N resonance assignments for wild-type and [C65S, C72S] mutant forms. Biochemistry 36(23):6915–6929. doi:10.1021/bi963024k

Wheeler TT, Maqbool NJ, Gupta SK (2012) Mapping, phylogenetic and expression analysis of the RNase (RNaseA) locus in cattle. J Mol Evol 74(5–6):237–248. doi:10.1007/s00239-012-9502-7

Wlodawer A, Borkakoti N, Moss DS, Howlin B (1986) Comparison of two independently refined models of ribonuclease-A. Acta Crystallogr B 42:379–387. doi:10.1107/S0108768186098063

Wong M, Khirich G, Loria JP (2013) What's in your buffer? Solute altered millisecond motions detected by solution NMR. Biochemistry. doi:10.1021/bi400973e

Zabrouskov V, Han XM, Welker E, Zhai HL, Lin C, van Wijk KJ, Scheraga HA, McLafferty FW (2006) Stepwise deamidation of ribonuclease A at five sites determined by top down mass spectrometry. Biochemistry 45(3):987–992. doi:10.1021/Bi0517584